JOURNAL OF GUIDANCE, CONTROL, AND DYNAMICS
Vol. 26, No. 4, July–August 2003

Stabilization of Helicopter Blades with Severed Pitch Links Using Trailing-Edge Flaps

Roberto Celi*
University of Maryland, College Park, Maryland 20742

The feasibility of using trailing-edge flaps to reconfigure a helicopter rotor blade following a failure of the pitch link is addressed, which makes the blade free floating in pitch and otherwise uncontrollable. A coupled rotor–fuselage model is developed that allows for rotor anisotropy. A new, optimization-based, trim procedure is developed to determine the dynamics of the failed blade and the flap inputs required for reconfiguration. The trailing-edge flap can correct the otherwise catastrophic consequences of a pitch link failure. The residual 1 and 2/rev (revolution) components of the hub loads are reasonably small with a one-harmonic flap input and essentially disappear if a second harmonic is added to the flap input. The required flap deflections are high but not unreasonable. The flap acts by generating a rigid-body pitching motion of the free-floating blade that matches the angles that otherwise would have been generated by the swashplate. The steady-state flapping motion of the reconfigured blade is very nearly identical to those of the undamaged blades. The solutions are very sensitive to phase errors in the first harmonic of the flap inputs. The sensitivity is lower for the constant and the second harmonic inputs. The result suggests that if a helicopter rotor is equipped with trailing-edge flaps for other purposes such as vibration or noise reduction, these flaps could be used as emergency control surfaces.

Nomenclature

I_{xx}, I_{yy}, I_{zz}	=	mass moments of inertia of the helicopter about its body axes
m	=	mass of the helicopter
$\boldsymbol{S}$	=	descent direction in optimization procedure for trim
X, Y, Z	=	components of hub forces, lbs
$\boldsymbol{X}$	=	vector of design variables in trim procedure
β	=	blade flapping angle
δ_F	=	flap deflection
μ	=	advance ratio (aircraft velocity divided by hover blade tip speed)
ϕ	=	rigid-body pitch of the failed blade
ψ	=	azimuth angle of the reference blade (blade number 1)
Ω	=	rotor speed

Subscripts and Superscript

nc	=	cosine component of nth harmonic
ns	=	sine component of nth harmonic
4	=	quantity for blade 4 (failed blade)

Introduction

IN recent years there has been a renewed interest in the use of trailing-edge flaps on the main rotor blades for noise and vibration reduction. Extensive theoretical research has been carried out, and model-scale tests have been performed. Full-scale experimentation is now under way. Recent studies representative of the state of the art in this area are those of Milgram and Chopra[1] and Myrtle and Friedmann.[2]

Trailing-edge flaps provide additional control effectors, besides the conventional swashplate controls. Therefore, they offer some degree of control redundancy and could potentially be used to reconfigure the rotor control chain in case of failures. Control reconfiguration has been successfully explored and tested in fixed-wing applications. However, the potential for helicopter applications has been severely limited by the lack of control redundancy, as shown by the few studies on this topic.

Aponso et al.[3] studied a case in which the roll swashplate actuator of a Sikorsky UH-60 is jammed or floating. No additional control surfaces were assumed, and reconfiguration was carried out through changes in the flight control laws. A simple linearized aircraft model was used. Huang et al.[4] considered a CH-47 tandem rotor configuration with combinations of jammed front and rear swashplate actuators. Reconfiguration was achieved through changes in the flight control laws. In one of the cases studied, some control redundancy was obtained by assuming that the rotational speeds of the rotors could be varied by up to $\pm 10\%$. A simple linearized six-degree-of-freedom (6-DOF) analysis model was used. In the only other published study on this topic, Heiges[5] considered a configuration representative of the AH-64 with all of the pitch links severed. Control was restored through the use of servoflaps installed on all of the blades. The study was based on a simple linearized rotor analysis.

The main objective of this paper is to study the dynamics and the reconfiguration of a single main rotor helicopter in which the pitch link of one of the blades has been severed, so that the blade is free floating in pitch. The reconfiguration is achieved through the use of a trailing-edge flap. The blade is schematically shown in Fig. 1. The specific problem that will be addressed is whether one can determine a flap control history that allows the trimming of the failed rotor and reduces the hub loads to acceptable levels. Because the focus of the study is simply to establish the theoretical feasibility of this type of reconfiguration, the control considered in this study is open loop only, and no feedback is considered.

The mathematical model is much more detailed than in the reconfiguration studies cited. It includes a full nonlinear, coupled rotor–fuselage dynamic model, from which a linearized, time-varying model can also be extracted. The anisotropy of the rotor, which has one blade with dynamics different from those of the other three, is fully taken into account. A new trim procedure is presented; the new procedure is required to deal with the rotor anisotropy and the flap control history.

Baseline Simulation Model

The mathematical model of the helicopter used in this study is a nonlinear blade-element-type model that includes fuselage, rotor,

Received 11 September 2000; revision received 17 March 2001; accepted for publication 24 March 2003.

*Associate Professor, Department of Aerospace Engineering, Alfred Gessow Rotorcraft Center; celi@eng.umd.edu. Senior Member AIAA.

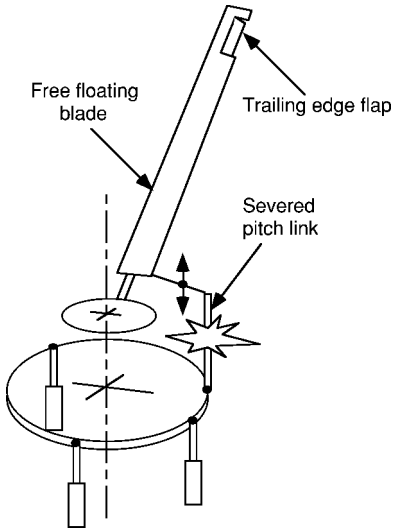

Fig. 1 Blade with severed pitch link and trailing-edge flap.

and main rotor inflow dynamics. The 6-DOF rigid-body motion of the aircraft is modeled using nonlinear Euler equations. Linear aerodynamics is assumed for fuselage and empennage. The blades are assumed to be rigid, with offset hinges and root springs. Flap and lag dynamics of each blade are modeled. The main rotor has four blades.

The coupled system of rotor, fuselage, and inflow equations of motion is written in first-order form. The state vector has a total of 28 elements: flap and lag displacements and rates for each of the 4 blades (16 states); 9 rigid-body velocities, rates, and attitudes; and 3 inflow states.

In the absence of a failure, the trim procedure is the same as in Ref. 6. Thus, the rotor equations of motion are transformed into a system of nonlinear algebraic equations using a Galerkin method. The algebraic equations enforcing force and moment equilibrium are added to the rotor equations, and the combined system is solved simultaneously. The solution yields the harmonics of a Fourier series expansion of the rotor DOF, the pitch control settings, the trim attitudes and rates of the entire helicopter, and the main and tail rotor inflow.

Modeling of the Failed Blade

The blade with the severed pitch link is assumed to be free floating in pitch as a rigid body. The flap and lag dynamic model remains otherwise unchanged. The inertia moments due to the motion of the flap are neglected. Therefore, the pitch equation of motion is simply

$$\ddot{\phi} + \Omega^2 \phi = M_\phi \tag{1}$$

where M_ϕ is the nondimensional aerodynamic pitching moment. The only aerodynamic pitching moment is that generated by the deflection of the trailing edge of the flap. The flap deflection $\delta_F(\psi)$ is assumed to have a harmonic variation, that is,

$$\delta_F(\psi) = \delta_0 + \sum_{n=1}^{N} (\delta_{nc} \cos n\psi + \delta_{ns} \sin n\psi) \tag{2}$$

with $\delta_F > 0$ for a downward deflection of the flap. The cases $N = 1$ and $N = 2$ will be considered in the present paper. The pitching moment coefficient c_{mF} is assumed to be linearly proportional to the flap deflection and is given by $c_{mF} = -0.64\delta_F$.

When the pitch link is severed, the swashplate pitch inputs are no longer applied to the blade. Therefore, the geometric angle of attack of the free-floating blade is given by the sum of the rigid-body pitch rotation ϕ and the geometric twist angle θ_B. This angle is used to calculate all of the aerodynamic forces acting on the blade (including the flap and lag dynamics).

Whereas the pitching model of the blade is probably adequate for a feasibility study, its limitations should be kept in mind. The most serious is the lack of unsteady aerodynamic modeling. Even in the absence of a trailing-edge flap, the motion of the airfoil introduces changes in both the magnitude and the phase of the lift, drag, and pitching moment coefficients; In particular, aerodynamic pitch damping is generated. The addition of the flap introduces further changes of the aerodynamic coefficients. A model such as that of Ref. 7 should be used for a more accurate representation of the unsteady aerodynamics of the flapped airfoil.

On the other hand, neglecting the elastic torsion of the free-floating blade may be a reasonable assumption for this study. In fact, for angular velocities typical of helicopter rotors, the frequency of the first elastic torsion mode of a rotating free–free beam is about twice that of the same beam cantilevered at the root. Typical frequencies of the fundamental elastic torsion mode are 3–6/rev (revolution), which implies that the response of the damaged blade at 1/ and 2/rev frequencies will be determined primarily by the rigid-body pitch mode.

From an aeroelastic stability point of view, the changes in lead–lag dynamics can probably be neglected, too, at least at the level of approximation used in the present study. It has been shown by Wang and Chopra[8] that small dissimilarities in rotor blade dynamics tend to increase the aeroelastic stability of the rotor. Therefore, if the dynamics of the reconfigured blade is close or identical to that of the other blades, the rotor should at least maintain the level of stability that it had before the failure. However, the assumption may not be as legitimate as far as the in-plane loads are concerned. In fact, the drag on the reconfigured blade might be substantially higher than that of the other blades, especially if large flap deflections are required. Therefore, any improved simulation of the reconfigured blade dynamics should carefully address the impact of neglecting lead–lag blade dynamics.

In summary, the coupled rotor–fuselage mathematical model consists of 30 nonlinear ordinary differential equations, namely, 9 Euler equations for rigid-body motion, 3 dynamic inflow equations, 2 equations for the flap and 2 for the lag dynamics of each of the 4 blades, and 2 pitch equations for the failed blade.

Trim Procedure for the Rotor with a Failed Blade

The trim procedure of Ref. 6 needs to be modified to take into account the damage to the blade. This is necessary for two primary reasons, namely, the rotor anisotropy and the need to determine the required flap trim control.

Treatment of Rotor Anisotropy

The free-floating blade has dynamics different from those of the other three blades, and therefore, it needs its own separate equations in the system of algebraic trim equations. Rigid-body flap and pitch dynamics of the free-floating blade are explicitly included in the trim procedure, whereas the lag dynamics are assumed to remain unchanged in trim. The flap and the pitch angles are represented in the form of a truncated Fourier series expansion, that is,

$$\beta^4(\psi) = \beta_0^4 + \sum_{n=1}^{2} \left(\beta_{nc}^4 \cos n\psi_4 + \beta_{ns}^4 \sin n\psi_4\right) \tag{3}$$

$$\phi^4(\psi) = \phi_0^4 + \sum_{n=1}^{2} \left(\phi_{nc}^4 \cos n\psi_4 + \phi_{ns}^4 \sin n\psi_4\right) \tag{4}$$

where the subscripts and superscripts 4 indicate that the failed blade is the fourth, with $\psi_4 = \psi + 270$ deg. Compared with the trim procedure of Ref. 6, there are new trim unknowns, namely, the coefficients of the preceding Fourier series. Therefore, anisotropy adds 10 unknowns to the trim problem. The corresponding 10 additional trim equations come from the application of Galerkin method (see

Ref. 6). For flap they are

$$\int_0^{2\pi} \varepsilon_{F4}(\psi)\,\mathrm{d}\psi = \int_0^{2\pi} \varepsilon_{F4}(\psi)\cos\psi\,\mathrm{d}\psi = \int_0^{2\pi} \varepsilon_{F4}(\psi)\sin\psi\,\mathrm{d}\psi$$

$$= \int_0^{2\pi} \varepsilon_{F4}(\psi)\cos 2\psi\,\mathrm{d}\psi = \int_0^{2\pi} \varepsilon_{F4}(\psi)\sin 2\psi\,\mathrm{d}\psi = 0 \quad (5)$$

where $\varepsilon_{F4}(\psi)$ is the residual obtained when the tentative trim solution is substituted into the flap equation of motion for the failed blade. Five similar equations are then written for the residual $\varepsilon_{P4}(\psi)$ of the blade pitch equation.

The total number of trim equations and unknowns for the case of the rotor with a failed blade case is 36. Besides the 10 unknowns just mentioned, the trim procedure yields values of the pitch settings of main rotor and tail rotor; fuselage angle of attack and sideslip angle; roll and pitch attitudes; roll, pitch, and yaw rates; and the harmonics of the steady-state flap and lag motions for the undamaged blades.

Determination of Flap Input

The coefficients δ_0, δ_{nc}, and δ_{ns} that describe the motion of the flap [Eq. (2)] cannot be directly added to the set of trim unknowns because there are no corresponding algebraic equations. Therefore, the trim formulation would consist of more unknowns than equations, and an infinite number of trim states would exist.

The solution devised for this study is to insert the baseline trim procedure in an unconstrained optimization loop. The vector $\boldsymbol{X}$ of design variables of the optimization consists of the coefficients of the flap motion:

$$\boldsymbol{X}^T = [\delta_0 \;\; \delta_{1c} \;\; \ldots \;\; \delta_{nc} \;\; \delta_{1s} \;\; \ldots \;\; \delta_{ns}] \quad (6)$$

Because the rotor is now anisotropic, multiblade load cancellations will not occur, and all harmonics of the hub loads will generally be present. If the generic hub force or moment component f is written in the form

$$f(\boldsymbol{X}) = f_0 + \sum_{n=1}^{2}(f_{nc}\cos n\psi + f_{ns}\sin n\psi) \quad (7)$$

the objective function to be minimized is

$$F(\boldsymbol{X}) = \left\{ \sum_{m=1}^{6}\sum_{n=1}^{2}\left[\left(f_{nc}^2\right)_m + \left(f_{ns}^2\right)_m\right]\right\}^{\frac{1}{2}} \quad (8)$$

where the subscript m is each of the three hub force and three hub moment components. In other words, the optimization loop seeks to minimize the coefficients of the 1 and 2/rev harmonics of all six hub components.

The resulting problem can be solved using any unconstrained minimization algorithm. In the present study the Fletcher–Reeves conjugate gradient algorithm (see Ref. 9) is used. Therefore, the improved value of the flap motion vector $\boldsymbol{X}_{k+1}$ is given by

$$\boldsymbol{X}_{k+1} = \boldsymbol{X}_k + \alpha^*\boldsymbol{S}_k \quad (9)$$

where α^* is the minimum of $F(\boldsymbol{X})$ along the direction $\boldsymbol{S}_k$, which is obtained from

$$\boldsymbol{S}_k = -\nabla F(\boldsymbol{X}_k) + \beta\boldsymbol{S}_{k-1} \quad \text{with} \quad \beta = \frac{\nabla F^T(\boldsymbol{X}_k)\nabla F(\boldsymbol{X}_k)}{\nabla F^T(\boldsymbol{X}_{k-1})\nabla F(\boldsymbol{X}_{k-1})} \quad (10)$$

where k is the iteration number and $\beta = 0$ for $k = 1$. Note that, for every value of $F(\boldsymbol{X})$ required during the optimization, a complete trim calculation is performed. The final solution consists of the vector $\boldsymbol{X}$ that minimizes the sum of the absolute values of all of the components of the 1 and 2/rev hub loads plus the corresponding values of all of the trim variables.

Note that the optimum harmonics of the flap motion obtained through the preceding trim procedure should be considered as ideal values that are valid for nonmaneuvering flight and that may not be necessarily achieved in an actual situation. In practice, the flap motion would be the output of some closed-loop control system, and the selection of sensors, actuators, and control law would clearly be key factors for a successful implementation of the concept. These important considerations will not be addressed, however, simply because the objective of the present study is limited to determining whether reconfiguration in such catastrophic failure conditions is at all possible.

Results

The results presented in this section refer to a soft-in-plane, hingeless rotor helicopter configuration roughly similar to a BO-105. The chordwise extension of the flap is 20% of the blade chord. The flap extends over the outermost 20% of the blade.

Figure 2 shows the iteration history of the objective function of the new trim procedure, that is, the rms value of the 1 and 2/rev components of the hub loads at an advance ratio $\mu = 0.15$. One iteration is defined as the calculation of one direction of descent $\boldsymbol{S}_k$ [Eq. (10)] and a one-dimensional minimization along $\boldsymbol{S}_k$ to obtain the new vector of flap coefficients $\boldsymbol{X}_{k+1}$ [Eq. (9)]. The direction finding problem requires the calculation of the gradient of the objective function and, therefore, four and six function evaluations for a one- and two-harmonic flap input, respectively. The one-dimensional minimization requires another two function evaluations besides the baseline to calculate an initial quadratic approximation. The minimum of the approximation is the candidate one-dimensional minimum and replaces the point with the highest value of the objective in the updated approximation. In all of the results of the present study, between three and five function evaluations were needed to achieve convergence on the one-dimensional minimum. Therefore, each iteration of the optimization-based trim procedure required a total of between 7 and 11 evaluations of the objective function $F(\boldsymbol{X})$ [Eq. (8)]. The initial guess for $\boldsymbol{X}$ in Fig. 2 is a zero vector, corresponding to an inactive flap. The trim procedure clearly converges quickly and reduces the hub loads by almost two orders of magnitude within the first iteration.

One-Harmonic Flap Input

Figure 3a shows the absolute values of the components of the 1 and 2/rev hub loads with the flap inactive; Fig. 3b shows the components with the flap activated, for the final iteration of the trim procedure. The advance ratio is again $\mu = 0.15$. All components should be equal to zero for a four-bladed rotor with identical blades and intact pitch links. Both sets of data refer to trimmed configurations. However, it is clear that for the rotor with the failed blade, "trim" is just a mathematical statement because the very large vibratory loads would quickly destroy the aircraft. The improvement brought about by the trailing-edge flap is dramatic: The peak values are reduced by almost three orders of magnitude.

The objective function is plotted in Fig. 4 as a function of advance ratio. Recall that the objective function is the square root of the sum of the squares of the first and second harmonics of the six hub load

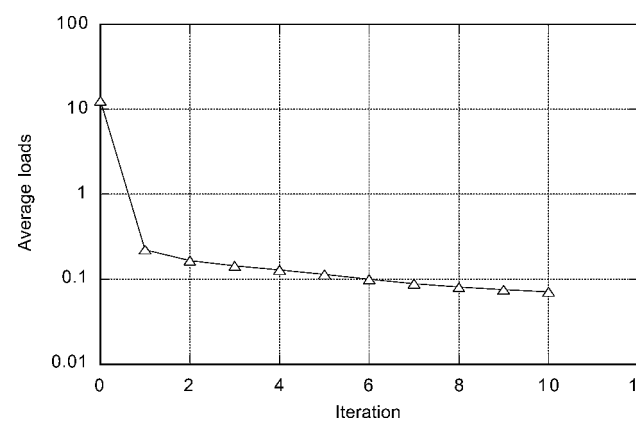

Fig. 2 Iteration history of the objective function of the trim procedure, $\mu = 0.15$.

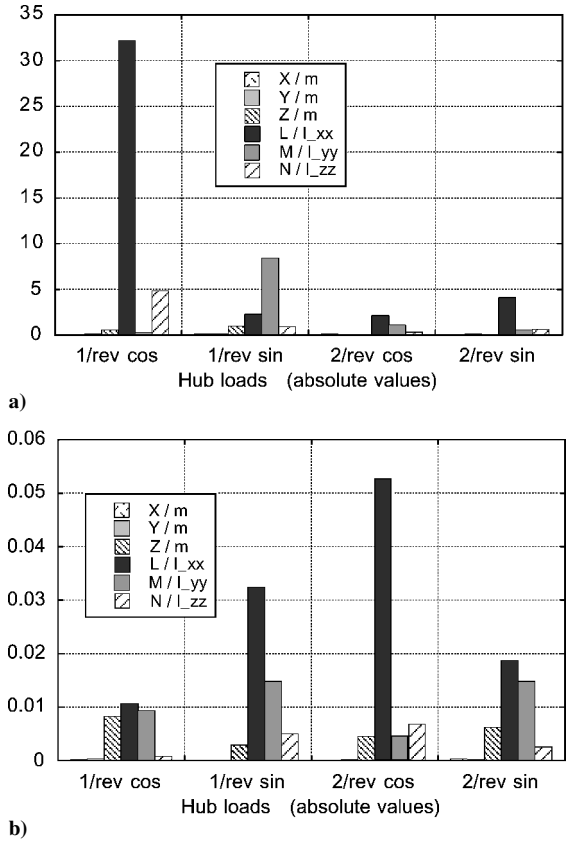

Fig. 3 One harmonic flap motion, $\mu = 0.15$, components of the hub loads a) without flap and b) with flap.

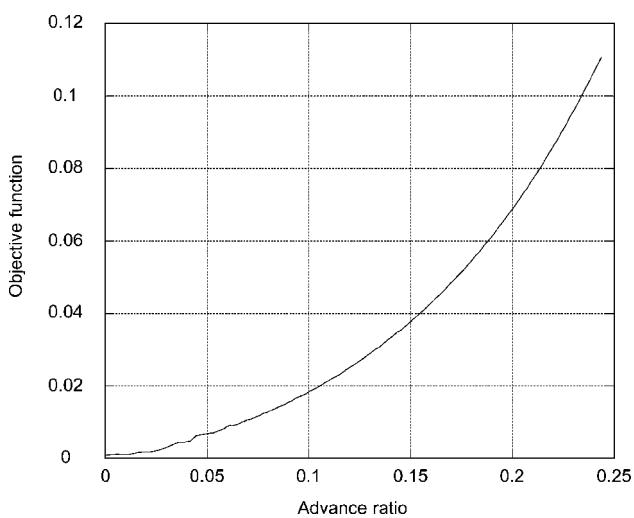

Fig. 4 Objective function as a function of advance ratio, one-harmonic flap motion.

components [Eq. (8)]. Although the residual loads increase almost quadratically with advance ratio, the flap clearly manages to contain them within reasonable limits.

The harmonics of the required flap motion are shown in Fig. 5 as a function of advance ratio. There is a constant, upward deflection of the flap of magnitude between 18.5 and 22 deg, depending on speed. Smaller first-harmonic motions are superimposed to it; their magnitudes are almost exactly zero at hover and slowly increase with speed. (A small amount of cyclic is needed in hover to counteract the effects of the tail rotor.)

The mechanism of action of the trailing-edge flap is evident from the results shown in Fig. 6. Figure 6 shows the value of collective and cyclic pitch settings as a function of advance ratio, plus the

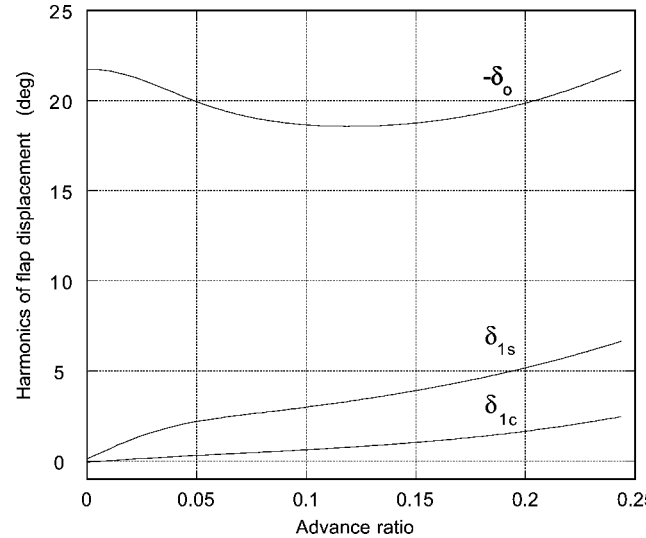

Fig. 5 Harmonics of flap motion as a function of advance ratio.

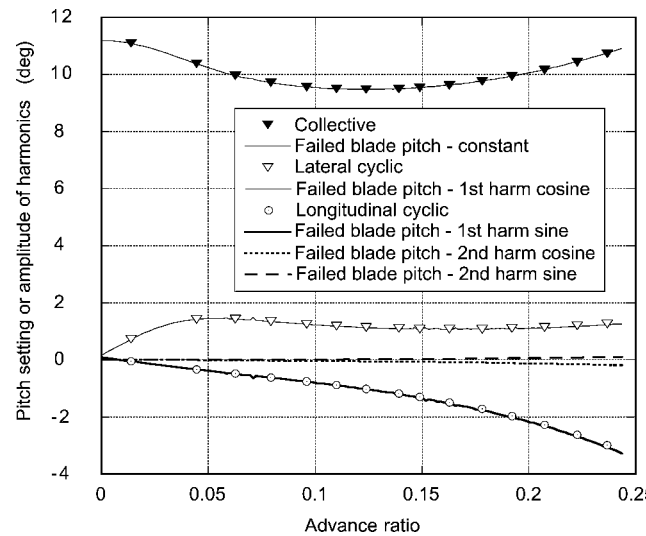

Fig. 6 Pitch settings and harmonics of rigid-body pitch motion of the failed blade as a function of advance ratio.

first two harmonics of the rigid-body pitching motion of the free-floating blade with the flap active. The constant harmonic of the pitch motion matches almost perfectly the collective pitch at every advance ratio. The same is true for lateral cyclic pitch and first harmonic cosine and for longitudinal cyclic pitch and first harmonic sine, respectively. The second harmonics of the rigid-body pitch are very small. Therefore, the trailing-edge flap acts in such a way that the dynamic pitch response of the blade matches the pitch angles that the swashplate controls would have generated, if the pitch link had not been severed. In retrospect, this conclusion may appear obvious. Note, however, that the optimization procedure used for trim explicitly includes neither the pitch dynamics of the failed blade nor the rotor pitch settings. The match between the two types of quantity is a byproduct of the attempt to minimize the 1 and 2/rev loads in the nonrotating system.

Because the action of the flap mimics almost perfectly the effect of the swashplate controls, the flap dynamics of the reconfigured blade are very close to that of the undamaged blades. This is clearly shown in Fig. 7, which is a comparison the first two harmonics of the flapping motion for both types of blades. Changes in lead–lag dynamics are neglected in this study, because the drag coefficient is assumed to be constant, and not affected by the flap motion. A more realistic flap model would have to take this effect into account: Drag changes will likely introduce 1/rev (and higher) lead–lag oscillations.

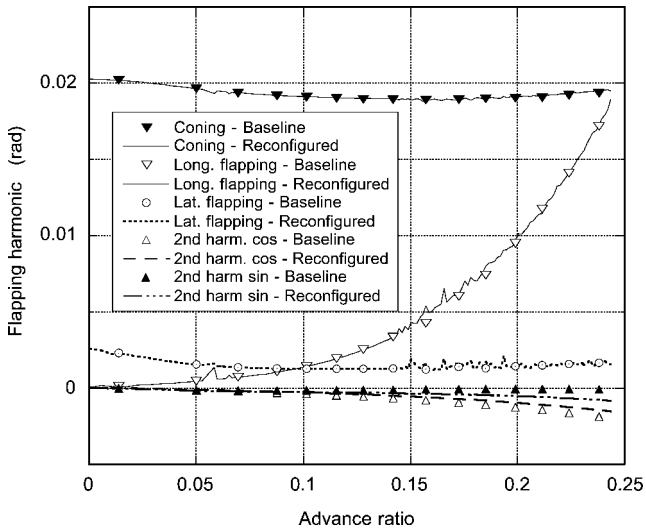

Fig. 7 Flapping harmonics for baseline and reconfigured rotors as a function of advance ratio.

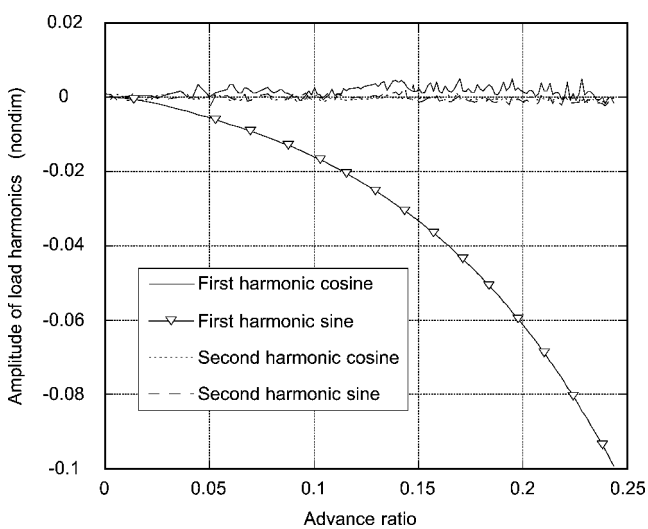

Fig. 8 Harmonics of roll moment as a function of advance ratio for the reconfigured blade.

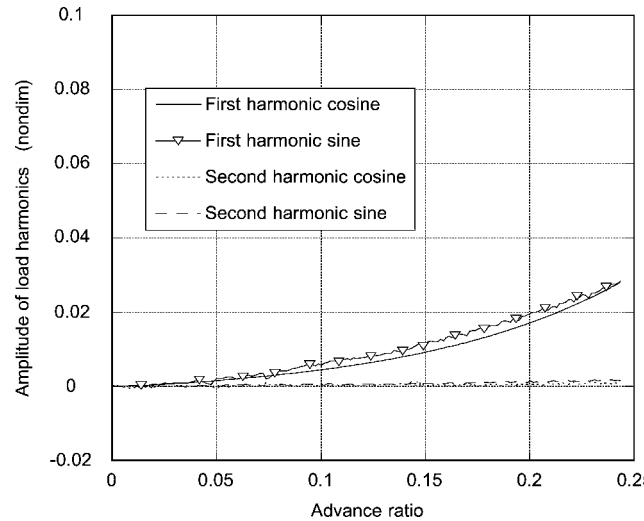

Fig. 9 Harmonics of pitch moment as a function of advance ratio for the reconfigured blade.

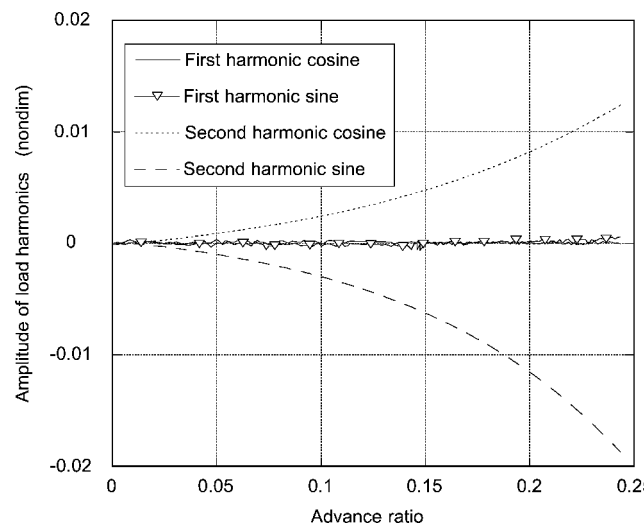

Fig. 10 Harmonics of Z force as a function of advance ratio for the reconfigured blade.

Figures 8–10 show the hub load components with the largest nondimensional values of unbalanced harmonics. Figure 8 shows the first and second harmonics of the roll moment as a function of advance ratio. The roll moment is normalized by dividing it by the roll moment of inertia of the helicopter. These harmonics are all equal to zero for the undamaged rotor. Figure 8 shows that the 1 and 2/rev harmonics are almost canceled by the flap, with the exception of the 1/rev sine component, which turns out to be the largest unbalanced component among all hub loads. The 1 and 2/rev harmonics of the pitching moment are shown in Fig. 9, which is drawn in the same scale as Fig. 8. The pitching moment of inertia of the helicopter is used for the normalization. The 1/rev sine and cosine harmonics have about the same size, whereas the 2/rev components are negligible. The pitch 1/rev components are the next largest hub load components. Figure 10 shows the harmonics of the Z force, nondimensionalized using the weight of the helicopter. For this hub load component, the 1/rev portion is negligible, whereas the 2/rev portion has the larger harmonics, which progressively increase with advance ratio.

Two-Harmonic Flap Input

Including a second harmonic in the trailing-edge flap input has a very substantial effect. This can be seen in Fig. 11, where the objective function is plotted as a function of advance ratio for the case of one- and two-harmonic flap input. Adding a second harmonic essentially reduces the value of the objective function to zero at all advance ratios considered. The harmonics of the corresponding flap inputs are shown in Fig. 12. The constant and first harmonic inputs are almost exactly the same as in the one-harmonic case.

Figure 13 shows the sine and cosine components of the second harmonics of the rigid-body pitch motion for the reconfigured blade, for one- and two-harmonic flap inputs. The curves for the one-harmonic flap input case are the same as in Figure 6, but here the scale of the vertical axis is expanded considerably. Clearly, introducing a second harmonic in the flap motion eliminates the second harmonic of the rigid-body pitching motion of the damaged blade at all advance ratios. Furthermore, with a two-harmonic flap input, the flapping dynamics of the reconfigured and the undamaged blades are identical, as shown in Fig. 14. The small discrepancies seen in Fig. 7 have been eliminated.

Features of the Optimization Problem

The trim state of the helicopter with the reconfigured blade is calculated using an optimization procedure. Because the underlying problem is nonlinear, the design space might be nonconvex, and local minima may exist. For a two-design-variable problem, it is possible to draw contours of constant values of the objective function

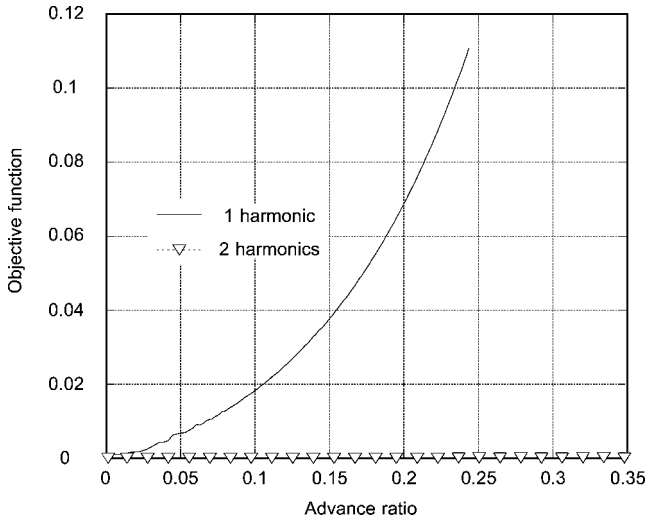

Fig. 11 Objective function as a function of advance ratio for one- and two-harmonic flap input.

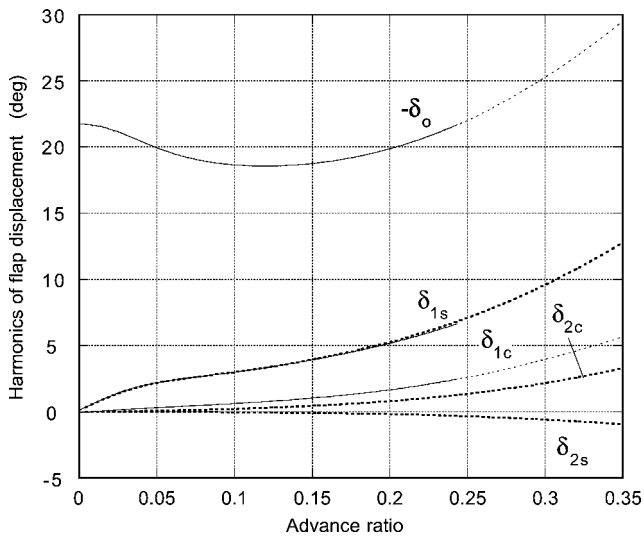

Fig. 12 Harmonics of flap motion as a function of advance ratio: ——, one-harmonic flap input and - - - -, two-harmonics flap input.

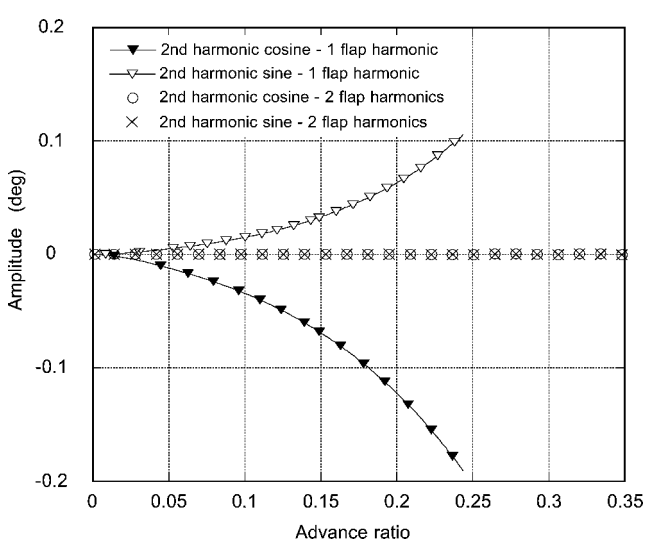

Fig. 13 Second harmonics of rigid-body pitch motion of the failed blade as a function of advance ratio; one- and two-harmonics flap input.

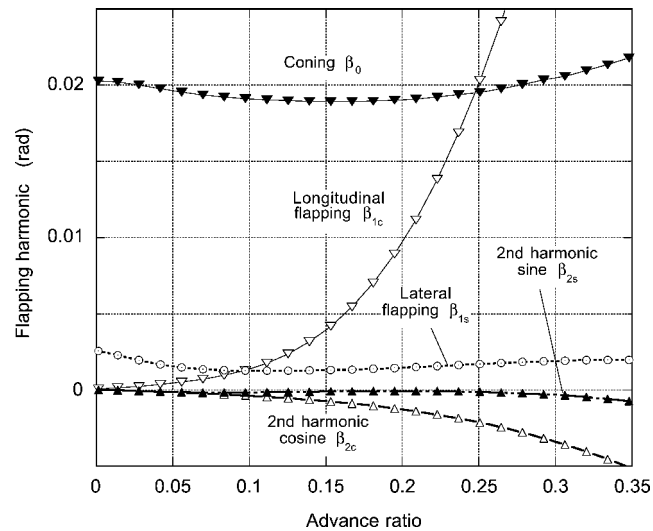

Fig. 14 Flapping harmonics for baseline and reconfigured rotors as a function of advance ratio: curves, reconfigured blade and symbols, undamaged blades.

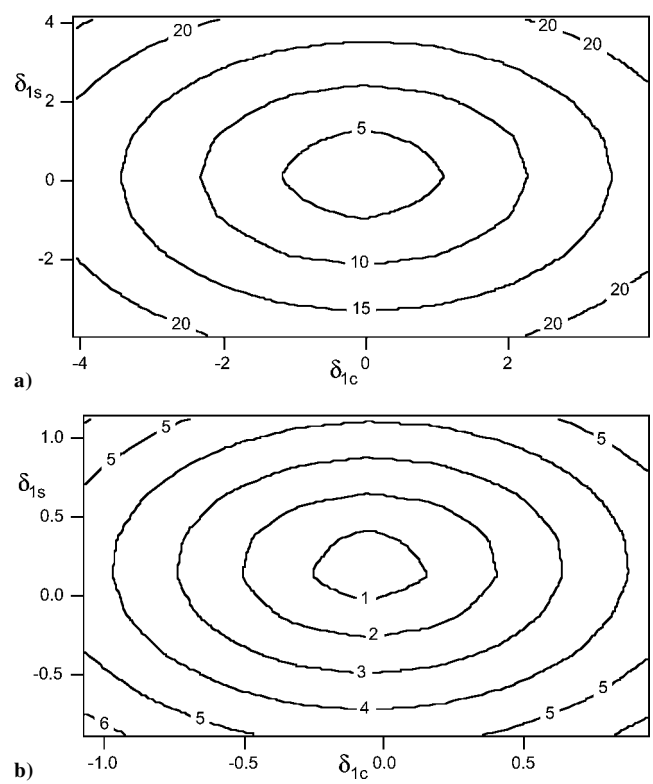

Fig. 15 Contours of constant objective function for one-harmonic flap case at two different scales (constant harmonic δ_0 held fixed at optimum value), hover.

and, therefore, study this issue directly. Figure 15 shows contour plots of the objective function for the one-harmonic flap case in hover. The constant flap input δ_0 is held fixed at its optimum value, and the first harmonics δ_{1c} and δ_{1s} are varied. In Fig. 15a, δ_{1c} and δ_{1s} are perturbed by up to ± 2 deg from their optimum values, in 0.5-deg increments. Figure 15b is more detailed, showing the neighborhood of the minimum, with perturbations of up to ± 1 deg in 0.25-deg increments. In both cases, the optimum is at the center of the plot. No local minima appear in Figs. 15, and the two-variable-design space appears to be well scaled. The same favorable behavior occurs in forward flight, at $\mu = 0.2$, as clearly shown in Fig. 16.

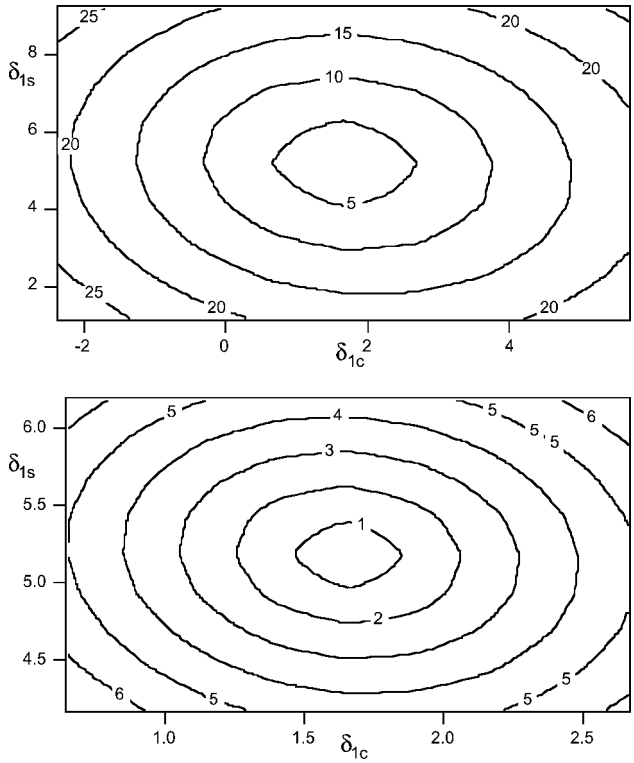

Fig. 16 Contours of constant objective function for one-harmonic flap case at two different scales (constant harmonic δ_0 held fixed at optimum value), advance ratio $\mu = 0.2$.

No contour plots can obviously be drawn for the two-harmonic flap problem, which has five unknowns (or design variables). Therefore, the existence of local minima was explored by repeating the optimization-based trim procedure with different initial guesses, which were obtained by perturbing in turn each component of the final solution by ±2 deg. The resulting 32 cases all converged to the same final solution, both in the case of hover and in forward flight with $\mu = 0.2$, indicating that multiple trim solutions should not be a practically important problem.

Sensitivity of the Optimum Flap Schedule

Finally, the robustness of the optimum trailing-edge flap schedule was studied by perturbing magnitude and phase of each input harmonic. The procedure consisted of 1) converting the accelerations at the center of gravity of the helicopter into linear accelerations at the pilot seat, under the assumption of a rigid fuselage, 2) computing the vector sum of the accelerations due to the 1 and 2/rev components of rotor vibrations, and 3) calculating the peak-to-peak values of the rms accelerations. The 1 and 2/rev components would be equal to zero for an isotropic rotor, and therefore, these peak-to-peak values provide an indication of the effectiveness of the trailing-edge flap.

Figure 17 shows the peak-to-peak rms accelerations as a function of the advance ratio for perturbations of ±0.25, ±0.5, and ±1 deg of the magnitude of the constant component of the flap deflection (Fig. 17a), first harmonic (Fig. 17b), and second harmonic (Fig. 17c). If a peak-to-peak value of 0.5 g is selected as a maximum practical limit, then Fig. 17 shows that an error of up to ±0.5 deg in the constant component is tolerable at all advance ratios, and one of ±1 deg is tolerable at lower speeds ($\mu \leq 0.15$). The first-harmonic input is very sensitive to magnitude errors, and only errors not much greater than ±0.25 deg can be tolerated. The second-harmonic input, on the other hand, is less sensitive, and an error of ±1 deg is acceptable. Figure 17 also shows that the peak-to-peak acceleration is an almost linear function of the perturbations and that positive and negative perturbations have almost identical effects.

Figure 18 shows the same type of results when it is the phase of the flap input to be perturbed. The phase perturbations are of ±5,

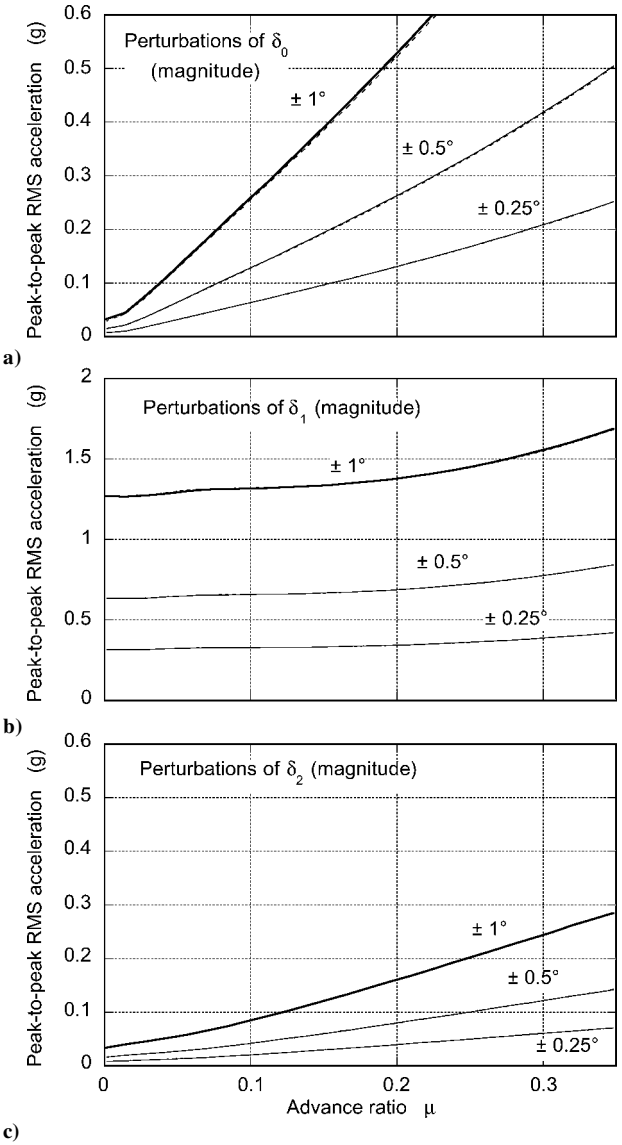

Fig. 17 Vibrations from 1 and 2/rev components when the magnitudes of the optimum flap schedules are perturbed.

±10, ±20, and ±40 deg for the first harmonic (Fig. 18a) and the second harmonic (Fig. 18b). The first-harmonic input appears to be extremely sensitive to phase errors. With an error of just ±5 deg, the practical limit of 0.5 g will be reached well below $\mu = 0.2$, and the situation will be considerably worse for larger phase errors. The second-harmonic input is far less sensitive, and errors of ±40 deg will be acceptable over most of the speed range.

Figures 17 and 18 also provide useful information on the sensitivity of the results of the present study to modeling assumptions. Because the 1/rev results are so sensitive to phase errors, as shown in Fig. 18, an accurate unsteady aerodynamic model will be especially important for reliable predictions. Equally important will be a correct prediction of the 1/rev flapping response. The 2/rev results, on the other hand, appear to be less sensitive to modeling errors. This confirms that it is probably reasonable to model the damaged blade as torsionally rigid.

Additional Comments

The simulation model used in this study contains several simplifying assumptions. These assumptions and their potential impact on the accuracy of the results have been addressed in various places of the present paper. However, a rotor with this type of anisotropy, including a free-floating blade, has never been studied in the literature. Therefore, any assessment of the accuracy of the model should be considered to some extent speculative.

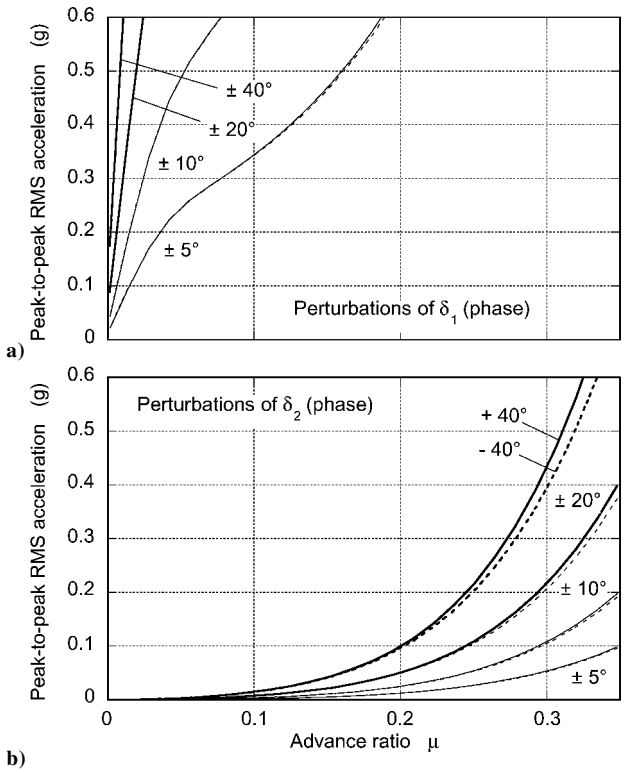

Fig. 18 Vibrations from 1 and 2/rev components when the phases of the optimum flap schedules are perturbed.

The modeling assumptions are such that the results of the study may be optimistic. For example, the simplified aerodynamic model with just linear inflow may lead to underestimating the vibratory loads. The trailing-edge flap will probably not maintain its full aerodynamic effectiveness at the higher deflections required at high speed. Its spanwise position is more outboard and its spanwise length is larger than those of the flaps currently envisaged for vibration or noise reduction.

On the other hand, consider the results of Fig. 3, which shows that the largest component of the residual hub loads following reconfiguration, namely, the 2/rev cosine harmonic of hub roll moment L, normalized by the roll moment of inertia of the helicopter I_{xx}, is slightly more than 0.05. This implies that the roll acceleration at 2/rev is slightly more than 0.05 rad/s^2, or about 3 deg/s^2 at 88 rad/s. If this hub load component is underestimated by a factor of 10, a 30-deg/s^2 angular acceleration at 2/rev can still be considered very reasonable for the reconfigured blade. Therefore, although a more conclusive assessment will require a more refined simulation model, the model of this study appears to be adequate for an initial feasibility study.

Conclusions

The feasibility is addressed of using trailing-edge flaps to reconfigure a helicopter rotor blade following a failure of the pitch link, which makes the blade free floating in pitch and otherwise uncontrollable. The problem was studied using a coupled rotor–fuselage model, which allowed for rotor anisotropy in the form of three identical blades with a dissimilar fourth. A new, optimization-based, trim procedure was developed to determine both the dynamics of the failed (and reconfigured) blade and the flap inputs required to achieve the best possible reconfiguration. A very simple aerodynamic model was used for the flap. Whereas the overall simulation model is probably adequate for a feasibility study, its limitations should be kept in mind when evaluating the quantitative conclusions of the study.

The results of the present study indicate the following:

1) The new optimization-basedtrim procedure is effective in calculating the trim state of the helicopter with the anisotropic rotor and in providing the stabilizing flap input. No local minima appear to exist for typical trim conditions.

2) The trailing-edge flap can correct the otherwise catastrophic consequences of a pitch link failure. The residual 1 and 2/rev components of the hub loads are reasonably small with a one-harmonic flap input and essentially disappear if a second harmonic is added to the flap input. The required flap deflections are high but not unreasonable.

3) The flap acts by generating a rigid-body pitching motion of the free-floating blade that matches at every azimuth the angles that would have been generated by the swashplate input, if the pitch link had not been severed. The steady-state flapping motion of the reconfigured blade is nearly identical to that of the undamaged blades.

4) The solutions are very sensitive to phase errors in the first harmonic of the flap inputs. The sensitivity is lower for the constant and the second-harmonic inputs.

5) The two most important refinements required for the mathematical model used in the present study are an unsteady aerodynamic model for the flap and the blades and an explicit modeling of the blade lead–lag dynamics. Modeling the torsional flexibility of the damaged blade is probably a lesser priority.

Overall, the results of the present study suggest that, if a helicopter rotor is equipped with trailing-edge flaps for other purposes such as vibration or noise reduction, these flaps could be used as emergency control surfaces to help reconfigure the flight control system following a failure or battle damage.

Acknowledgments

This research was supported by the National Rotorcraft Technology Center, under the Rotorcraft Center of Excellence Program, Technical Monitor Yung Yu.

References

[1]Milgram, J. H., and Chopra, I., "Rotors with Trailing-Edge Flaps: Analysis and Comparison with Experimental Data," *Journal of the American Helicopter Society*, Vol. 43, No. 4, 1998, pp. 319–331.

[2]Myrtle, T. F., and Friedmann, P. P., "Vibration Reduction in Rotorcraft Using the Actively Controlled Trailing Edge Flap and Issues Related to Practical Implementation," *Proceedings of the 54th Annual Forum of the American Helicopter Society*, American Helicopter Society, Alexandria, VA, 1998, pp. 602–619.

[3]Aponso, B. L., Klyde, D. H., and Mitchell, D. G., "Development of Reconfigurable Flight Controls for Helicopters," Systems Technology, Inc., Rept. STI TR-1295-1, Hawthorne, CA, 1997.

[4]Huang, C. Y., Celi, R., and Shih, I.-C., "Reconfigurable Flight Control Systems for a Tandem Rotor Helicopter," *Journal of the American Helicopter Society*, Vol. 44, No. 1, 1999, pp. 50–62.

[5]Heiges, M., "Reconfigurable Controls for Rotorcraft—A Feasibility Study," *Journal of the American Helicopter Society*, Vol. 42, No. 3, 1997, pp. 254–263.

[6]Celi, R., "Hingeless Rotor Dynamics in Coordinated Turns," *Journal of the American Helicopter Society*, Vol. 36, No. 4, 1991, pp. 39–47.

[7]Hariharan, N., and Leishman, J. G., "Unsteady Aerodynamics of a Flapped Airfoil in Subsonic Flow by Indicial Concepts," *Journal of Aircraft*, Vol. 33, No. 5, 1996, pp. 855–868.

[8]Wang, J. M., and Chopra, I., "Dynamics of Helicopters with Dissimilar Blades," *Proceedings of the 47th Annual Forum of the American Helicopter Society*, American Helicopter Society, Alexandria, VA, 1991, pp. 1399–1412.

[9]Vanderplaats, G. N., *Numerical Optimization Techniques for Engineering Design: With Applications*, McGraw–Hill, New York, 1984, Chap. 3.